



RESEARCH ARTICLE

Ultrastructure and stability of cellular nanoparticles isolated from *Phaeodactylum tricornutum* and *Dunaliella tertiolecta* conditioned media [version 1; peer review: awaiting peer review]

Darja Božič^{1,2}, Matej Hočevar³, Marko Jeran ^{1,2}, Matic Kisovec ⁴, Apolonija Bedina Zavec⁴, Anna Romolo¹, David Škufca¹, Marjetka Podobnik⁴, Ksenija Kogej ⁵, Aleš Iglič^{2,6}, Nicolas Touzet⁷, Mauro Manno ⁸, Gabriella Pocsfalvi ⁹, Antonella Bongiovanni¹⁰, Veronika Kralj Iglič ¹

¹Laboratory of Clinical Biophysics, Faculty of Health Sciences, University of Ljubljana, Ljubljana, SI-1000, Slovenia

²Laboratory of Physics, Faculty of Electrical Engineering, University of Ljubljana, Ljubljana, SI-1000, Slovenia

³Department of Physics and Chemistry of Materials, Institute of Metals and Technology, Ljubljana, SI-1000, Slovenia

⁴Department of Molecular Biology and Nanobiotechnology, National Institute of Chemistry, Ljubljana, SI-1000, Slovenia

⁵Faculty of Chemistry and Chemical Technology, University of Ljubljana, Ljubljana, SI-1000, Slovenia

⁶Faculty of Medicine, University of Ljubljana, Ljubljana, Slovenia

⁷Centre for Environmental Research Innovation and Sustainability, Institute of Technology SLIGO, Sligo, F91 YW50, Ireland

⁸Cell-Tech Hub, Institute of Biophysics, National Research Council of Italy, Palermo, Italy

⁹Extracellular Vesicles and Mass Spectrometry Group, Institute of Biosciences and BioResources, National Research Council of Italy, Palermo, Italy

¹⁰Institute of Biosciences and Bioresources, National Research Council of Italy, Palermo, Italy

V1 First published: 20 Oct 2022, **2**:121
<https://doi.org/10.12688/openreseurope.14896.1>

Latest published: 20 Oct 2022, **2**:121
<https://doi.org/10.12688/openreseurope.14896.1>

Abstract

Background: Cells in general secrete nanoparticles (NPs) which are believed to mediate intercellular communication. Recently, great efforts have been made to utilize them as delivery vectors. We aimed to harvest and identify NPs from liquid cultures of two marine microalgae *Dunaliella tertiolecta* and *Phaeodactylum tricornutum*.

Methods: NPs were isolated from the culture conditioned media by differential ultracentrifugation by the protocol used for the isolation of extracellular vesicles. Microalgae and isolated NPs were examined by scanning electron microscopy (SEM) while isolated NPs were examined also by cryogenic transmission electron microscopy (cryo-TEM). The Triton X-100 detergent and temperature sensitivity of NPs was assessed by dynamic light scattering (DLS) through monitoring the intensity of the scattered light (I) and the distribution of hydrodynamic radii of NPs (R_h).

Results: Two mechanisms of formation of NPs with average R_h 200

Open Peer Review

Approval Status AWAITING PEER REVIEW

Any reports and responses or comments on the article can be found at the end of the article.

nm were observed in the *D. tertiolecta* culture: a disintegration of tubular protrusions, and cell decay. A part of the imaged *D. tertiolecta* NPs were membrane-enclosed vesicles, but the isolates also contained electron-dense NPs and nanofilaments. *P. tricornutum* NPs in the culture and in the isolate were homogeneous in size and shape. Their average R_h was 104 nm. The addition of surfactant to isolates resulted in a change in R_h distribution and a decrease of I in samples from both species, indicating decay of a part of NPs. Changes in the width of the $I(R_h)$ peaks were observed at temperatures above 45 °C. **Conclusions:** A part of NPs found in isolates from microalgae *D. tertiolecta* and *P. tricornutum* were membrane-enclosed vesicles. However, the isolates obtained by a standard protocol for extracellular vesicle isolation by ultracentrifugation contained also a significant amount of other similar-sized nanoparticles. The isolates were partly susceptible to the addition of detergent and to temperature up to 80 degrees.

Keywords

Nanoalgosomes; Extracellular vesicles; Small cellular particles; Cellular nanoparticles; Exosomes; Electron microscopy of extracellular vesicles; Characterization of extracellular vesicles; Microalgae



This article is included in the [Cell, Molecular and Structural Biology](#) gateway.

Corresponding author: Veronika Kralj Igljč (veronika.kralj-iglic@fe.uni-lj.si)

Author roles: **Božič D:** Conceptualization, Data Curation, Formal Analysis, Investigation, Methodology, Visualization, Writing – Original Draft Preparation, Writing – Review & Editing; **Hočevar M:** Data Curation, Investigation, Methodology, Visualization, Writing – Review & Editing; **Jeran M:** Data Curation, Investigation, Writing – Review & Editing; **Kisovec M:** Data Curation, Investigation, Methodology, Writing – Review & Editing; **Bedina Zavec A:** Investigation, Methodology, Visualization, Writing – Review & Editing; **Romolo A:** Data Curation, Investigation, Writing – Original Draft Preparation, Writing – Review & Editing; **Škufca D:** Data Curation, Investigation, Writing – Review & Editing; **Podobnik M:** Funding Acquisition, Methodology, Resources, Visualization, Writing – Review & Editing; **Kogej K:** Formal Analysis, Funding Acquisition, Investigation, Methodology, Resources, Validation, Writing – Original Draft Preparation, Writing – Review & Editing; **Igljč A:** Funding Acquisition, Investigation, Project Administration, Resources, Writing – Review & Editing; **Touzet N:** Investigation, Methodology, Project Administration, Writing – Review & Editing; **Manno M:** Investigation, Methodology, Project Administration, Resources, Writing – Original Draft Preparation, Writing – Review & Editing; **Pocsfalvi G:** Funding Acquisition, Investigation, Methodology, Project Administration, Resources, Validation, Visualization, Writing – Original Draft Preparation, Writing – Review & Editing; **Bongiovanni A:** Conceptualization, Funding Acquisition, Methodology, Project Administration, Resources, Writing – Review & Editing; **Kralj Igljč V:** Conceptualization, Data Curation, Formal Analysis, Funding Acquisition, Investigation, Methodology, Project Administration, Resources, Supervision, Validation, Visualization, Writing – Original Draft Preparation, Writing – Review & Editing

Competing interests: No competing interests were disclosed.

Grant information: This project has received funding from the European Research Council (ERC) under the European Union's Horizon 2020 research and innovation programme (grant agreement No 801338); and the Slovenian Research Agency (ARRS projects P3-0388, P2-0132, P2-0232, P1-0391, L3-2621, J3-3066).

The funders had no role in study design, data collection and analysis, decision to publish, or preparation of the manuscript.

Copyright: © 2022 Božič D *et al.* This is an open access article distributed under the terms of the [Creative Commons Attribution License](#), which permits unrestricted use, distribution, and reproduction in any medium, provided the original work is properly cited.

How to cite this article: Božič D, Hočevar M, Jeran M *et al.* **Ultrastructure and stability of cellular nanoparticles isolated from *Phaeodactylum tricornutum* and *Dunaliella tertiolecta* conditioned media [version 1; peer review: awaiting peer review]** Open Research Europe 2022, 2:121 <https://doi.org/10.12688/openreseurope.14896.1>

First published: 20 Oct 2022, 2:121 <https://doi.org/10.12688/openreseurope.14896.1>

Plain language summary

The Future and Emerging Technologies (FET) Open Horizon 2020 project Ves4Us funded by EU Commission investigated nanoalgsomes that were isolated from conditioned media of microalgae. It was our aim within this project, to identify NPs in isolates and reveal the mechanisms of their formation. Here we present our findings on material isolated from the conditioned media of two marine microalgae: *Dunaliella tertiolecta* and *Phaeodactylum tricornutum*. We have applied cryogenic transmission electron microscopy (cryo-TEM) and scanning electron microscopy (SEM) to assess their morphology. We have assessed the susceptibility of NPs to surfactant (Triton X-100) and to temperature by using dynamic light scattering (DLS). We have found NPs in conditioned media and in isolates from conditioned media of both microalgal species. Some of them were membrane-enclosed vesicles. The NPs were partly susceptible to surfactant Triton X-100 and to the increase in the temperature in the range between 10°C and 80 °C.

Introduction

Extracellular vesicles (EVs) are membrane-enclosed particles released by cells that have recently gained increasing attention because of their role in cellular communication¹⁻⁴, and we have already published a recent paper in this area^{1,2}. EVs have been recognized as a means of effective intercellular communication for their particular structure: the lipid-based membrane encloses the cargo and transfers proteins, DNA, and RNA between neighbouring or distant cells. Due to their high biocompatibility, limited immunogenicity, and higher stability compared to synthetic vesicles, EVs have been investigated as potential drug delivery systems⁵. To obtain a material with optimal properties, methods are being developed to engineer and produce nanoparticles (NPs) with well-defined properties from natural sources⁶. Plant-derived NPs are being considered as a convenient source due to their immunomodulatory, antitumor, and regenerative activities⁷, and have been shown to deliver functional exogenous proteins into human cells⁸. Recent works^{1,2} proposed microalgae as a promising renewable source of EVs (named nanoalgsomes) with potential use as new generation biogenic nanocarriers of bioactive molecules.

However, the underlying mechanisms of EV formation and action are not yet fully understood. EV isolates usually contain a spectrum of submicron-sized materials with overlapping physicochemical properties⁹. It is therefore a challenge to define the composition, properties and biological activity of the individual components, the interplay between them and the basic mechanisms of NPs formation.

In microalgae, the production of membranous NPs has already attracted the attention of researchers a few times in the past. Thin tubular membrane protrusions and EVs were isolated from the conditioned medium of *Ochromonas danica*¹⁰⁻¹², in *Chlamydomonas sp.*, formation of flagellar EVs was observed during gamete mating¹³⁻¹⁵, and in *Emmilia huxleyi*, increased production of EVs modulating the host-virus dynamics was noted during viral infection¹⁶. Recently, a systematic study of microalgal NPs was performed in search of the organisms with

an optimal yield of NPs¹. The expression “nanoalgsomes” has been introduced². The marine microalgae *Tetraselmis chuii* (*T. chuii*) has been characterized in detail² and the ability of NPs to transfer material to the recipient cells has been demonstrated². However, as microalgae are a group of very different organisms, the physiological roles and dynamics of nanoalgsome production in different phyla remain unexplored.

In this work, we focused on two cultures of marine unicellular algae - a green flagellate without a cell wall - *Dunaliella tertiolecta* (*D. tertiolecta*) and an atypical pennate diatom *Phaeodactylum tricornutum* (*P. tricornutum*)¹. We harvested extracellular material from conditioned media by differential centrifugation, according to methods commonly used for the isolation of extracellular vesicles¹⁷. Samples were examined using scanning electron microscopy (SEM) and cryogenic transmission electron microscopy (cryo-TEM) to reveal the structure of the isolated NPs and collect some evidence of their formation and release.

While electronic microscopy is key in the identification of particles in the samples and reveals their size and shape, complementary information on the samples is provided by the methods which assess the averages over a very large number of NPs in the samples. Dynamic light scattering (DLS) gives information proportional to the abundance and size of NPs by means of the intensity of the scattered light I , and hydrodynamic radius R_h . NPs stability was assessed by changes in I and in R_h distribution that reflect the influence of the sample conditions (i.e. addition of surfactant Triton X-100 and increase of the temperature) on the NPs.

Methods

Design of the study

Microalgae were cultured in a respirometer with controlled temperature, air ventilation and light. NPs were isolated by differential ultracentrifugation as described in detail below. Microalgal cultures and isolates from conditioned media were fixed with osmium and analyzed by SEM to inspect the surface structure and the three-dimensional shape of particles. NP isolates were analysed also by cryo-TEM to inspect the NPs' ultrastructure. The size of limited number of NPs was estimated from the electron micrographs while the size distribution of a very large population of NPs was estimated by their R_h determined by DLS. The sensitivity of NPs to Triton X-100 and to temperature was assessed by DLS by monitoring I and R_h .

Cultivation of the algae

Cultures of *D. tertiolecta* CCAP 19/22, and *P. tricornutum* CCAP 1052/1A from the Culture Collection of Algae and Protozoa (CCAP) of SAMS (Oban, Scotland) were grown in artificial seawater (Reef Crystals, Aquarium Systems, France). A total of 22 g of salt was dissolved in one litre of distilled water, sterile filtered (0.2-micron cellulose filters, ref. 11107-47-CAN, Sartorius Stedim Biotech GmbH, Germany), autoclaved, and supplemented with Guillard's (F/2) Marine Water Enrichment Solution (ref. G0154, Sigma Aldrich, USA)¹⁸. Cultures were grown in a respirometer (Echo, Slovenia)

in 0.5-L borosilicate bottles, at 20 °C and 20 % illumination (approximately 250 $\mu\text{mol}/\text{m}^2\text{s}$) with a 14-hour light / 10-hour dark cycle, with aeration of 0.2 L/min.

Isolation of nanoparticles (NPs)

NPs were isolated by differential centrifugation, using a protocol widely used for the isolation of EVs¹⁶. Briefly, the cells were removed by low-speed centrifugation (300 g, 10 min, 4°C, centrifuge Centric 260R with rotor RA 6/50 (Domel, Slovenia)), using 50 mL conical centrifuge tubes (ref. S.078.02.008.050, Isolab Laborgeräte GmbH, Germany); and 2000 g, 10 min, 4°C (Centric 400R centrifuge with rotor RS4/100 (Domel, Slovenia)), using 15 mL conical centrifuge tubes (ref. S.078.02.001.050, Isolab Laborgeräte GmbH, Germany). Each step was repeated twice. Then, the cell-depleted medium was centrifuged twice at 10 000 g and 4°C for 30 min (Beckman L8-70M ultracentrifuge, rotor SW55Ti (Beckman Coulter, USA)), using thin-wall polypropylene centrifuge tubes (ref. 326819, Beckman Coulter, USA) to remove larger cell debris. Finally, NPs were pelleted by ultracentrifugation at 118 000 g and 4°C, for 70 min in the same type of ultracentrifuge and ultracentrifuge tubes. The isolate (i.e. pellet of NPs after differential ultracentrifugation) obtained from about 30 mL of conditioned media was not visible by eye. For assessment, the isolates were suspended in artificial seawater.

Scanning Electron Microscopy (SEM)

Samples were fixed according to our previously published protocol (see ref. 4). They were loaded onto 0.05-micron Mixed Cellulose Ester (MCE) filters (MF-Millipore™, ref. VMWP01300) and incubated in 2% OsO₄ for two hours. Then the osmium was removed, and the filter was taken out from the holder and further treated in a 24-well plate by changing the bath solution. After washing three times in distilled water, the samples were dehydrated in a graded series of ethanol (30%, 50%, 70%, 80%, 90%, absolute), treated with hexamethyldisilazane (30%, 50% mixtures with absolute ethanol, followed by pure hexamethyldisilazane), and air-dried. Samples were sputtered with Au/Pd (PECS Gatan 682) and examined with a JSM-6500F Field Emission Scanning Electron Microscope (JEOL Ltd., Tokyo, Japan).

Cryogenic Electron Microscopy (Cryo-TEM)

For Cryo-TEM, samples of NPs isolates were prepared by using Vitrobot Mark IV (Thermo Fisher Scientific, Waltham, MA, US). Quantifoil® R 2/2 (or 1.2/1.3), 200 mesh holey carbon grids (Quantifoil Micro Tools GmbH, Großlobbichau, Germany) were glow discharged at 20 mA for 60 s and at positive polarity in the air atmosphere (GloQube® Plus, Quorum, Laughton, UK). Conditions were set at 95% relative humidity, 4 °C, blot force: 4 and blot time: 5 s. 2 μL of the sample containing nanoparticles in suspension was applied to the grid, blotted, and vitrified in liquid ethane. Samples were visualized under cryogenic conditions. A 200 kV microscope Glacios with Falcon 3EC detector (Thermo Fisher Scientific, Waltham, MA, US) was used.

Dynamic Light Scattering (DLS)

The average hydrodynamic radius (R_h) of NPs and the average intensity of light (I) scattered from NPs in the samples were

assessed for characterization of NPs by Dynamic Light Scattering (DLS). The value of I was interpreted as a measure of NP concentration (in the case of preserved particle size distribution) or as a topological change (in the case of altered particle size distribution)^{18,19}. For analysis of the samples we used Instrument 3D-DLS-SLS cross-correlation spectrometer from LS Instruments GmbH (Fribourg, Switzerland) with a 100 mW DPSS laser (Cobolt Flamenco, Cobolt AB, Sweden) having a wavelength $\lambda_0 = 660$ nm. Before measurements, samples were equilibrated in a decalin bath at 25 °C for 15 min. The scattered light was measured at an angle $\theta = 90^\circ$ for 120 s. The correlation functions and integral time-averaged intensities $I(\theta) \equiv I(q)$ (where q is the scattering vector, defined as $q = (4\pi n_0 / \lambda_0) \sin(\theta/2)$, with n_0 the refractive index of the medium, in our case estimated by the corresponding value for water, i.e. $n_0 = 1.33$ at 25°C and λ_0 the wavelength of the light), were recorded simultaneously. The R_h values of NPs were obtained from the diffusion coefficients (D) that were assessed from the correlation function of the scattered electric field ($g_1(t)$). The $g_1(t)$ function was calculated from the measured correlation function of the scattered light intensity $g_2(t)$ by applying Siegert's relation^{20,21} (please find the values of $g_2(t)$ in the files linked as given in the *data availability* section at the end of the manuscript). To convert D to R_h , the Stokes-Einstein equation was used ($R_h = kT/6\pi\eta D$, where k is the Boltzmann constant, T is the absolute temperature, and η is the viscosity of the medium, in which the particles diffuse). It was assumed that particles have a spherical shape. The viscosity of the medium was not known. We approximated the viscosity value to that of water at 25°C. The analysis was carried out using an in-house created software based on the inverse Laplace transform program CONTIN. The in-house software performs the same functions as the program CONTIN. The code for the program CONTIN (freely available [here](#)). was accessed 25. 1. 2011. We collected several intensity correlation functions for each setting. Curves were analyzed independently and compared with the averaged curve. The correlation curves were fitted with up to 50 exponents.

To test the effect of Triton X-100 on NPs, 0.1% (V/V) of Triton X-100 was added to the sample before the measurement. The change in R_h distribution and the change of scattered light intensity ($\Delta I = I_{\text{sample}} - I_{\text{sample}+0.1\% \text{ TritonX-100}}$) was determined. Thermal stability analysis was performed using the Litesizer™ 500 instrument (Anton Paar GmbH). Samples were heated from 15 °C to 80 °C in 5 °C steps. When the target temperature was reached the samples were equilibrated for another 5 minutes before 10 measurements of 20 s duration were performed. The size distributions were determined from the mean correlation function using the program Kalliope™, Version 2.16.0 (Anton Paar GmbH), applying the CONTIN approach. A new version of Kalliope™ 4.12.0 is freely available online [here](#).

Results

SEM analysis of *D. tertiolecta* and *P. tricorntutum* cells and respective NPs

Figure 1 shows SEM images of *D. tertiolecta* cells (Panels a-f) and of the respective NPs isolated from the conditioned media (Panels g,h). The cells of *D. tertiolecta* have two flagella (Panel a) but exhibited also tubular protrusions of different

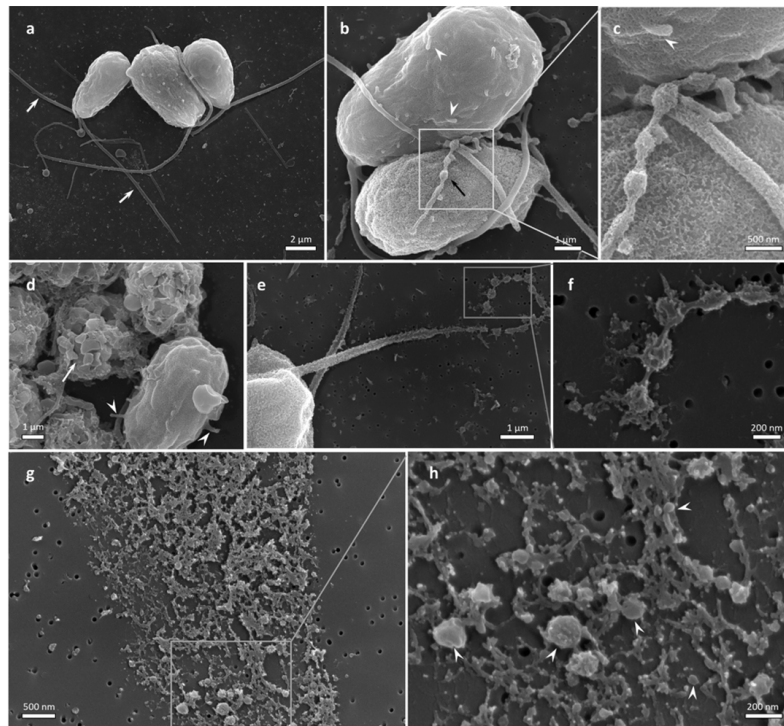


Figure 1. SEM visualization of *D. tertiolecta* cell culture and of NP isolates from the respective conditioned media. **a:** *D. tertiolecta* cells (white arrows point to flagella), **b:** *D. tertiolecta* cells with short tubular protrusions (white arrowheads) and long undulated tubular structure adhered to the cell body (black arrow). **c:** Close-up of a part of the beaded protrusion. The white arrowhead points to a short protrusion. **d:** Group of decaying cells (white arrow), and a cell with short protrusions (white arrowheads point to two of the protrusions), **e:** Fragmenting flagellum, **f:** Higher magnification image of the fragmenting part of the flagellum, **g:** NPs isolated by differential centrifugation, **h:** Higher magnification image of a selected region (some globular nanoparticles are marked with white arrowheads).

lengths (Figure 1b–d). Most of these protrusions were shorter than 1 μm (Figure 1b–d, white arrowheads). Dead cells disintegrated into irregularly shaped chunks (Figure 1d, white arrow). In isolates, globular particles (Figure 1h, white arrowheads) were enclosed in deposits of amorphous material (Figure 1g,h). The undulation of the tubular structures (e.g. flagella) and their decomposition into pearls were observed (Figure 1b (black arrow) and c,e,f).

Figure 2 shows SEM images of *P. tricoratum* cells and NPs in the culture (Panels a–e) and the isolate from conditioned media (Panels f and g). The cells were mostly in fusiform shape (Panels a,d). While some of the observed NPs of different sizes had smooth surfaces (Panel c), numerous NPs in the isolate were homogeneous in shape and size (Panel f). The estimated average size of NPs in the isolate was between 50 and 200 nm (Panel g). NPs tended to cluster into groups (Panels b,c,f,g). In some cells, nanostructures with rough surface were observed on epitheca (Panels d and e).

Cryo-TEM analysis of NPs isolates from *D. tertiolecta* and *P. tricoratum* conditioned media

Cryo-TEM of isolates from the *D. tertiolecta* conditioned media revealed the presence of membrane-enclosed vesicles

(Figure 3a; white arrowheads), double-lined elongated structures (Figure 3a; twin arrows, Figure 3f–h), and electron-dense globular structures of different sizes (Figure 3a,b, black arrowheads; and Figure 3e). A close-up shows a membrane coat formed by radially oriented fibres, reaching the width of the coating up to 50 nm (Figure 3 c,d).

Cryo-TEM of the *P. tricoratum* isolates indicated the presence of membrane-enclosed vesicles decorated by a coat of radially oriented fibres (Figure 4a–d, white arrowheads) and electron-dense NPs (Figure 4a,b,e; black arrows). The sample was abundant with long nanofilaments (Figure 4b, white arrow; and Figure 4e) and short branched nanofilaments (Figure 4b,e, black arrowheads). On a close-up, a zigzag form of the long nanofilaments (Figure 4f) and a branched form of short nanofilaments (Figure 4g) could be observed.

Stability analysis of NPs by DLS

The results of NP stability analysis by DLS are summarized in Figure 5 and Figure 6. Figure 5 shows the effect of adding the surfactant Triton X-100 to the isolates and Figure 6 shows the effect of temperature T on the position and height of the main peak.

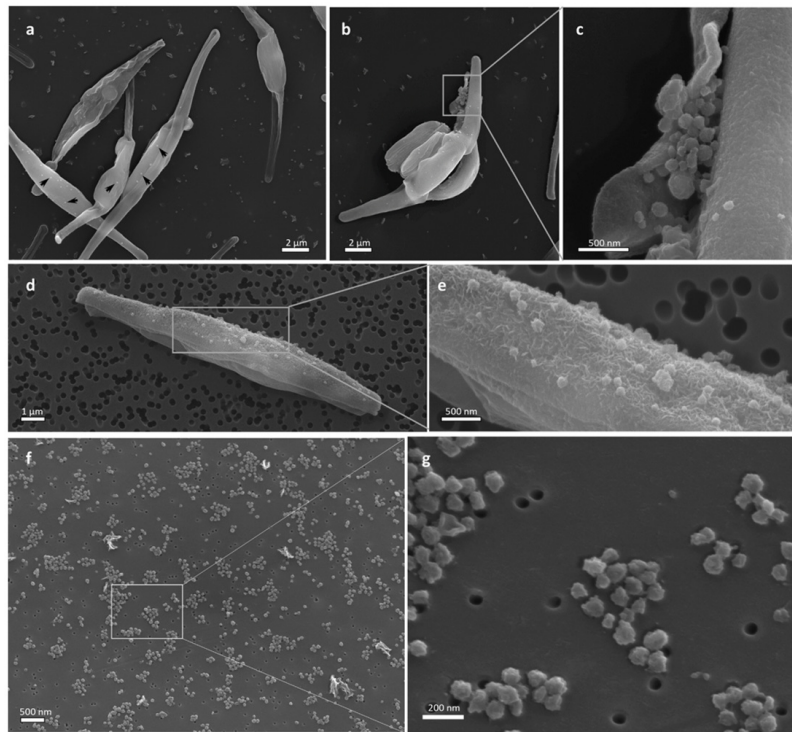


Figure 2. SEM visualization of *P. tricorutum* in cell culture and of NP isolates from the conditioned media. **a:** *P. tricorutum* fusiform cells with NPs on the surface (some are marked with black arrowheads), **b:** A cluster of NPs on the cell surface, **c:** Higher magnification image of the region, **d:** Fusiform cell with many nanostructures on the epitheca, **e:** Higher magnification image of the region, **f, g:** Isolate from conditioned media.

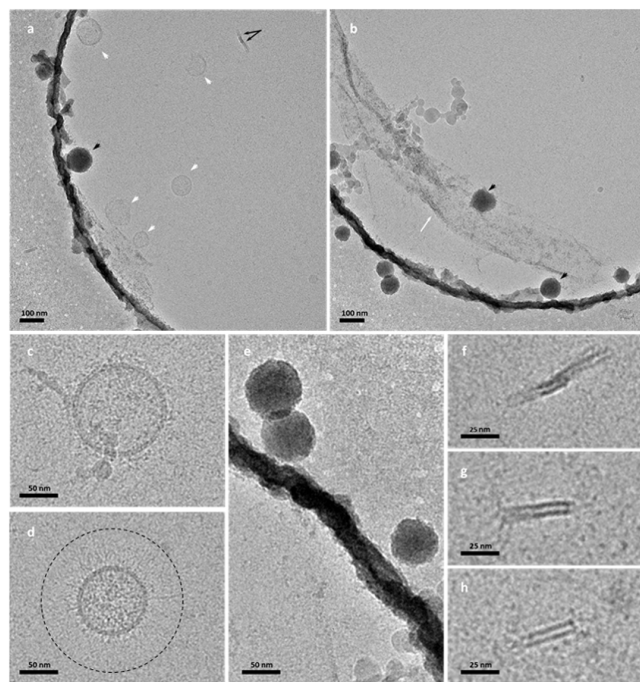


Figure 3. Cryo-TEM visualization of NP isolates from the *D. tertiolecta* cell culture conditioned media. **a:** Membrane enclosed spherical vesicles (white arrowheads), electron-dense spherical structure (black arrowhead), and double-lined elongated structure (black twin arrows); **b,e:** Electron dense spherical structures (black arrowheads) and deposited amorphous material (white arrow); **c,d:** Membrane coat formed on membrane-enclosed vesicles, dashed-lined circle in **(d)** surrounds the coat of radially oriented fibres; **f-h:** Double-lined elongated structures.

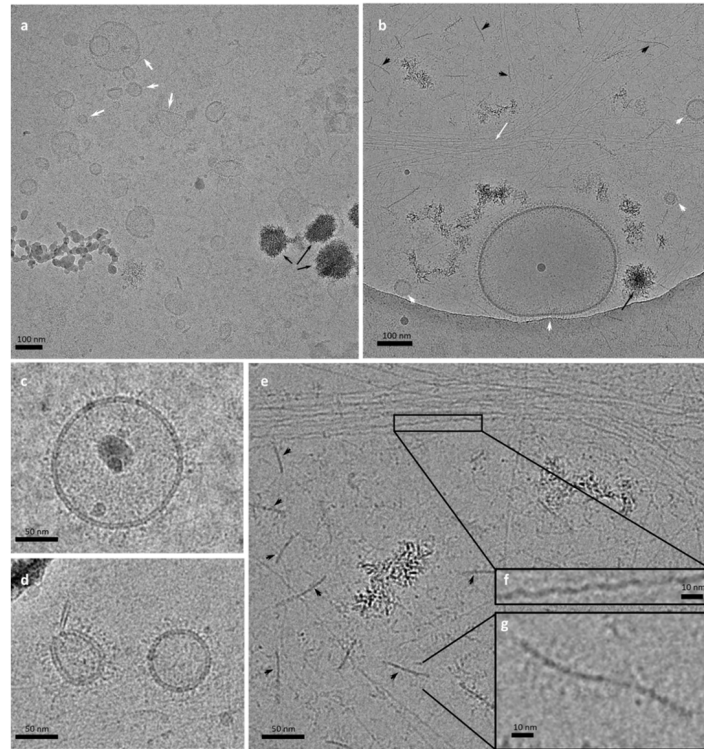


Figure 4. Cryo-TEM visualization of NP isolates from the *P. tricorutum* conditioned media. **a:** Numerous membrane-enclosed spherical vesicles (white arrowheads) and electron-dense clusters (black arrows); **b:** Membrane-enclosed vesicles (white arrowheads), electron-dense clusters (black arrow), long nanofilaments (white arrow) and shorter branched nanofilaments (black arrowheads); **c,d:** High magnification images of nanovesicles with a coat of radially oriented fibres; **e:** Electron dense NPs, long nanofilaments and shorter branched nanofilaments (black arrowheads); **f:** Close-up on the zigzag form of long nanofilaments **g:** High magnification image of a short branched nanofilament.

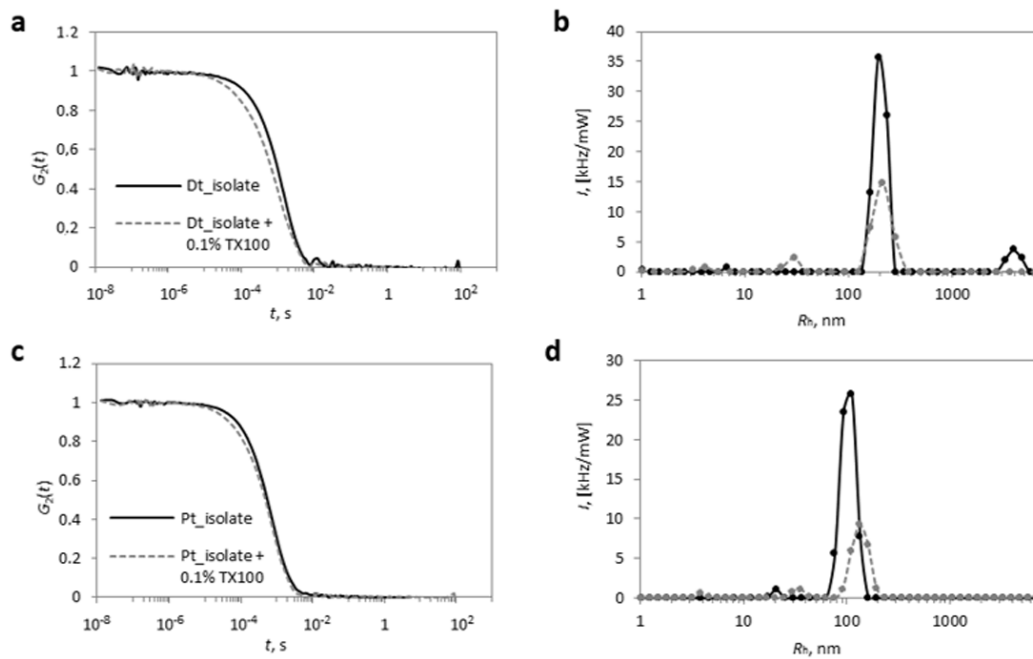


Figure 5. The normalized correlation functions ($G_s(t)$: Panels **a,c) and the calculated distributions of I over R_h (Panels **b,d**) before (full black lines) and after (dashed grey lines) the addition of the surfactant Triton X-100 (TX100) at a concentration of 0.1 % to isolates from conditioned media of *D. tertiolecta* (**a,b**) and *P. tricorutum* (**c,d**).**

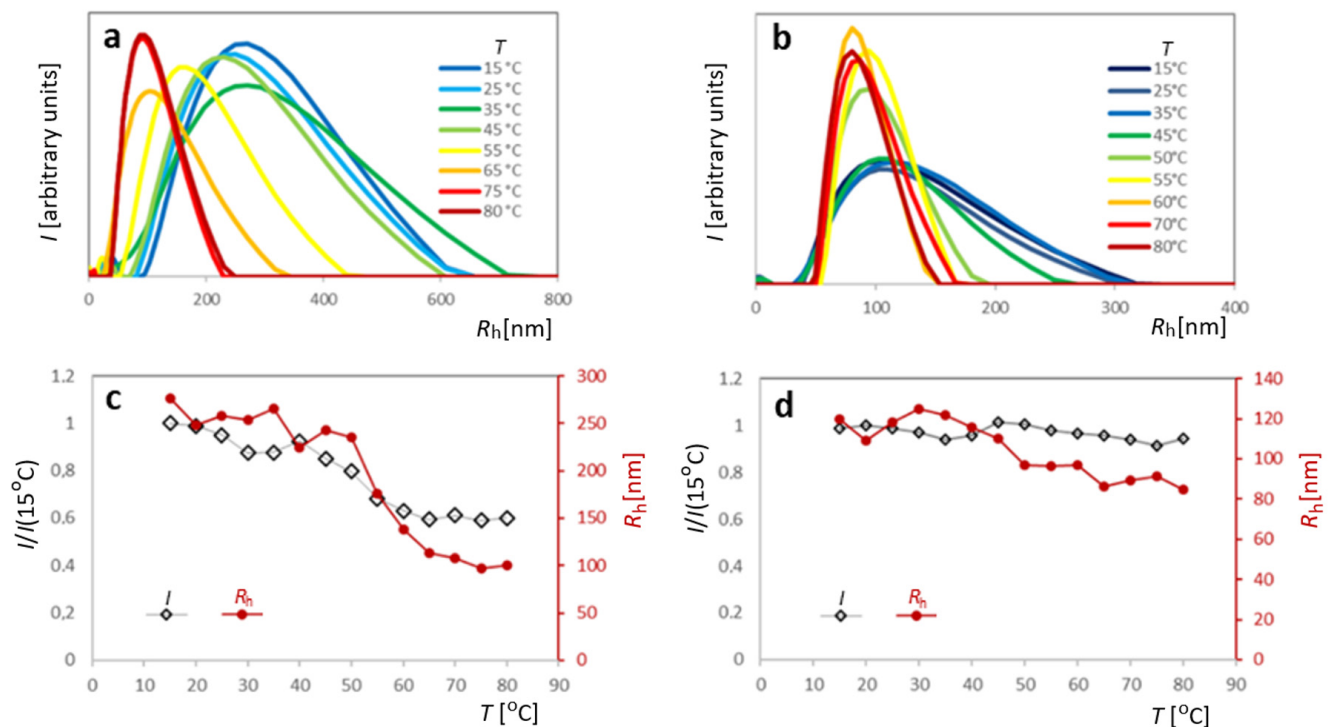


Figure 6. Effect of temperature T on the stability of NPs in isolates from conditioned media of *D. tertiolecta* (a,c) and *P. tricorutum* (b,d). a, b - the distribution of I over R_h for different T . c, d - dependence of I (normalized to the initial value measured at 15 °C) on T . For clarity, only the dependencies $I(R_h)$ pertaining to 8 (in *D. tertiolecta*, Panel a) and 9 (*P. tricorutum*, Panel b) different temperatures are shown. Dependencies $I(T)$ are presented by open black diamonds with the scale on the primary (left-side) axis, and dependencies $R_h(T)$ are presented by full red circles with the scale on the secondary (right-side) axis. The data points are connected to show the progression of the results.

Representative (intensity weighted) R_h distributions for isolates from *D. tertiolecta* and *P. tricorutum* mostly display 3 peaks in the nanometre size range (Figure 5). The population with the highest contribution to I is the one with mean R_h values between 100 and 200 nm (*c.f.* the highest or the main peak). Particles with mean R_h below 10 nm and around 20 nm were the most numerous ones (number distributions not shown). Also particles with mean R_h larger than 1 μm (mostly around 10 μm ; not shown in Figure 5) were found in the samples.

The mean R_h value in the isolate from *D. tertiolecta* conditioned media was ~ 200 nm and in the isolate from *P. tricorutum* conditioned media was ~ 100 nm (Table 1). Low values of I (< 100 kHz/mW) indicated a low number of NPs in the isolates of both species (Figure 5b,d and Table 1). Treatment of isolates with 0.1% Triton X-100 resulted in a loss of more than half of the original I (Table 1) and lead to a broadening of the distribution with a concomitant shift to slightly higher mean R_h values (Figure 5b,d). This was more evident in the case of *P. tricorutum* (Figure 5b: the mean R_h value for *P. tricorutum* was shifted from 104 nm to 140 nm). The shape of the correlation functions $G_2(t)$ at shorter correlation times t , *i.e.* in the initial part (compare the full black and the dashed grey lines in Figures 5a and b), indicated that Triton X-100 caused some degradation of NPs

into smaller particles and simultaneous formation of larger particles.

Figure 6 shows the effect of an increase in temperature on the R_h distributions. Note that R_h distributions are not normalized in these plots. In the case of *D. tertiolecta* (Panels a and c), the height of the peak of the R_h distribution was not significantly affected by T . However, an increase in T shifted the curves to lower mean R_h values and lead to a narrowing of the size distributions with a concomitant decrease in total scattering intensity (Figure 6c). The decrease in I was steeper at temperatures above 40°C, which was accompanied by a significant decrease in R_h values (Figure 6c). In *P. tricorutum*, the effect of temperature was different. The main peak of the size distribution was broader at temperatures below 50°C and the peak height was lower (Figure 6b). However, the total intensity of the scattered light remained constant throughout the temperature interval and the mean R_h values decreased only gradually (Figure 6d).

Discussion

Intercellular communication and modulation of the local milieu are fundamental to increasing cell survival and thus are important drivers of organismal evolution. Studies of cell secretions help us to understand cell physiology, including mechanisms of resistance (adaptation to environmental

Table 1. Stability parameters of NPs (mean hydrodynamic radius of the main peak R_h , corresponding intensity of the scattered light I and relative change of the intensity I due to the addition of the detergent Triton X-100 $\Delta I/I$) in the isolates from conditioned media of *D. tertiolecta* and *P. tricornutum* as determined by DLS.

	R_h [nm]	I [kHz/mW]	$(\Delta I/I) \times 100$ (0.1% Triton X-100)
<i>D. tertiolecta</i>	200	72	-61 %
<i>P. tricornutum</i>	104	52	-54 %

stresses) and opportunistic proliferation. Peri-membrane components, such as glycocalyx-imposed forces may contribute to the formation and the regulation of the size and shape of EVs²².

The scientific community is beginning to understand the importance of NPs in cell-to-cell communication. Of these, sub-micron-sized membrane-enclosed particles that cannot replicate (EVs) are of special interest and are gaining increasing attention⁸. In addition to their numerous important biological functions, NPs' physicochemical properties make them promising tools for the fine-tuned delivery of biologically relevant compounds³. However, for efficient and safe application, knowledge about their mechanisms of action should be deepened.

Following characterization of nanoalgsomes from *Tetraselmis chuii*², we here present new results (cryo-EM morphological analysis, and stability assessment) on nanomaterial from *D. tertiolecta* and *P. tricornutum*. Our results show that isolates from both species contain membrane-enclosed vesicles decorated with a coat formed by radially oriented fibers of various extensions (Figure 3a,c,d, and Figure 4a–d), but also other types of NPs. SEM images of NPs isolated from *P. tricornutum* conditioned media (Figure 2 and Figure 4, respectively) revealed numerous particles homogeneous in size and shape (Figure 2c–g).

The estimated diameters of vesicles observed by SEM in our samples (Figure 1g,h, Figure 2c–g) were between 50 nm and 200 nm and the average R_h of NPs in isolates were 200 nm in *D. tertiolecta* and 104 nm in *P. tricornutum*. It is expected, that the intensity-weighted distribution (I over R_h) is inclined towards larger particles, due to their stronger light scattering properties. In a previous report¹, the nanoalgsomes in the isolates from conditioned media of *D. tertiolecta* and *P. tricornutum* had mean diameters of 160 nm and 90 nm, respectively, (determined by NTA), while intensity-weighted mean hydrodynamic diameters (determined by DLS) were approximately 400 nm and 200 nm, respectively.

We observed two types of globular particles within this size interval in the images of isolates from *P. tricornutum* by cryo-TEM: membrane-enclosed vesicles and electron-dense NPs (Figure 4a–d). Shape, size, and surface roughness of structures observed on the epitheca of some cells in the culture

(Figure 2d,e) seem similar to NPs with rough surface found in isolate (Figure 2f,g) which indicates that the mechanism of formation of these particles could be budding of the cell wall (Figure 2d,e). It was previously shown that peri-membrane features, such as glycocalyx-imposed forces may contribute to the formation of NPs, and the regulation of the size and shape of EVs²². As the frustule has a well-ordered structure, the uniform size of the buds and the NPs could be indicated. Considering that the *P. tricornutum* frustule contains silica-containing material it can be expected that they would appear electron-dense in cryo-TEM (Figure 4a). As for EVs, it remains unclear how would the vesicles with a coat of radially oriented fibers (Figure 4a) be imaged by SEM. Also we did not observe indications of the mechanism of formation of membrane-enclosed EVs that were found in the isolate (Figure 4a).

The NP isolates (from both species) contained besides EVs also other types of NPs. Most notably, long filaments and shorter branched nanofilaments can be seen in isolates from *P. tricornutum* (Figure 4b,e). Structurally similar extracellular components (e.g. polysaccharides²³, proteoglycans^{24,25}) can be found in complex tissues of multicellular organisms.

Budding of the cell surface was observed in the study by Silverman *et al.* (2008), who examined the secretions of the kinetoplastid *Leishmania donovani*²⁶. Globular buds in *Leishmania* cells were evenly distributed over the entire cell surface during the transformation from promastigote to amastigote²⁶. The authors confirmed the presence of orthologous proteins characteristic for EVs released from eukaryotic cells²⁶. Several glycolytic enzymes were detected in their isolates²⁶, possibly related to the mechanisms of polysaccharide cell coating restructuring required for vesicle release and uptake. Buds of *P. tricornutum* in culture (Figure 2d,e) were of similar size and shape, however, of different surface roughness.

We found vesicles in isolates from *D. tertiolecta* conditioned media, however, not in a sufficient quantity to consider them a prevalent type in the isolates. Under the influence of various stress factors (e.g. hypoosmotic surroundings), the cells of *D. tertiolecta* form giant vesicles²⁷. In SEM images, NPs have diverse shapes (Figure 1d), and such shapes have not been indicated by the minimum of the membrane free energy²⁸.

According to SEM and cryo-TEM, isolates from *D. tertiolecta* were significantly poorer in vesicles than isolates from *P. tricorutum* while DLS indicated higher I and larger R_h in isolates from *D. tertiolecta* culture conditioned media than in respective isolates from *P. tricorutum* (Table 1). This could be explained by the presence of larger aggregates found in the SEM of the isolates from *D. tertiolecta* (Figure 1h) as well as by the thick fibrous layer visible on the cryo-TEM images (Figure 2 f,g, Figure 4a), contributing to the increased hydrodynamic radii of the decorated NPs. Namely, the presence of larger particles causes stronger scattering of light despite of their smaller number in the sample.

In general, susceptibility of NPs in the isolates to transformation by surfactants, specifically Triton X-100, indicates the key role of the membrane in contrast to the role of protein complexes of similar size²⁹. Different populations of vesicles have different susceptibilities to lysis with surfactants, but according to the study by Osteikoetxea *et al.*³⁰, 0.1 % Triton was expected to solubilize most of them. By using DLS we found that approximately 40 % of the material in the isolates from both species was resistant to degradation with 0.1 % Triton X-100 (Table 1). Partial resistance to detergents was previously observed also in isolates from microalgae *T. chuii*². As many topologically distinct particles were observed in our isolates, the possible varying impact of detergents on them would need further examination.

Loss of I was accompanied by a shift in R_h distribution toward higher R_h values in both types of microalgae (Figure 5b,d). Upon heating, the distributions narrowed towards smaller R_h at temperatures above 45°C in isolates from conditioned media of both types of microalgae (Figure 6a,b). In *D. tertiolecta*, the effect of temperature was also evident from the decrease in average I and R_h values above ~45°C (Figure 6c), whereas in *P. tricorutum*, I and R_h remained approximately constant (I) or decreased slightly (R_h) within the temperature range examined (Figure 6d).

All three techniques used (SEM, cryo-TEM, and DLS) are subjected to limitations. The isolation procedure and preparation for SEM and cryo-TEM may considerably affect specific types of NPs. Preparation of samples for SEM imaging involves drying of the samples which may shrink the vesicles; in cryo-TEM, the vesicles get squeezed within a thin layer of ice and albeit they preserve their closed structure, they may be flattened and presented by a deformed contour; DLS does not measure the size of the particles but instead, their average effective hydrodynamic radius in motion (that is with a weight proportional to the form factor and the square of the mass). Presently available methods for NP isolation, identification, and characterization are limited due to the complexity, fragility, and transient identity of the material, as well as due to the small size of the particles considered. Observation of nano-sized particles is beyond the use of optical microscopy and requires preparation of the samples for electron microscopy which may however cause

profound changes in their structure. Advanced technological solutions and further study of the mechanisms of formation of NPs are needed.

Ethics and consent

Ethical approval and consent were not required.

Data availability

Underlying data

Zenodo: Scanning electron microscope images of *Dunaliella tertiolecta* and *Phaeodactylum tricorutum* cultures and scanning electron microscope images and cryogenic electron microscope images of isolated small cellular particles from respective conditioned media, <https://doi.org/10.5281/zenodo.6908895>³¹.

Zenodo: Raw data on dynamic light scattering assessment of small cellular particles isolated from conditioned culture media of *Dunaliella tertiolecta* and *Phaeodactylum tricorutum*. Effect of Triton X-100 and temperature, <https://doi.org/10.5281/zenodo.7016692>³².

This underlying data contains 34 data files:

- The files: DLS raw data *Dunaliella tertiolecta* isolate.csv and DLS raw data *Dunaliella tertiolecta* isolate TX100.csv pertain to the species *D. tertiolecta* (plain samples and samples with added detergent Triton X-100).
- The files: DLS raw data *Phaeodactylum tricorutum* isolate.csv and DLS raw data *Phaeodactylum tricorutum* isolate TX100.csv pertain to the species *P. tricorutum* (plain samples and samples with added detergent Triton X-100).
- The files: Dt_isolate_temperature_sensitivity_overal.csv and Pt_isolate_temperature_sensitivity_overal.csv pertain to the summed up data on the temperature sensitivity analysis of *D. tertiolecta* and *P. tricorutum* isolates, respectively.
- The files: Dt_isolate_temperature_sensitivity_TX(YoC).csv and Pt_isolate_temperature_sensitivity_TX(YoC).csv where X stands for the number of sample and Y stands for the temperature in degrees (Celsius), pertain to *D. tertiolecta* and *P. tricorutum* isolates, respectively. There were 14 different temperatures considered, pertaining to 14 files for each species of microalgae.

Data are available under the terms of the [Creative Commons Attribution 4.0 International license](#) (CC-BY 4.0).

Software availability

The DLS analysis was performed by using the program Kalliope™, Version 2.16.0 (Anton Paar GmbH), applying the CONTIN approach. The version 2.16.0 is not freely available but the new version of Kalliope™ 4.12.0 is freely available online [here](#).

References

- Piccio S, Barone ME, Fierli D, et al.: **Isolation of extracellular vesicles from microalgae: towards the production of sustainable and natural nanocarriers of bioactive compounds.** *Biomater Sci.* 2021; **9**(8): 2917–2930. [PubMed Abstract](#) | [Publisher Full Text](#)
- Adamo G, Fierli D, Romancino DP, et al.: **Nanoalgosomes: Introducing extracellular vesicles produced by microalgae.** *J Extracell Vesicles.* 2021; **10**(6): e12081. [PubMed Abstract](#) | [Publisher Full Text](#) | [Free Full Text](#)
- Yáñez-Mó M, Siljander PR, Andreu Z, et al.: **Biological properties of extracellular vesicles and their physiological functions.** *J Extracell Vesicles.* 2015; **4**(1): 27066. [PubMed Abstract](#) | [Publisher Full Text](#) | [Free Full Text](#)
- Božič D, Hočevar M, Kisovec M, et al.: **Stability of Erythrocyte-Derived Nanovesicles Assessed by Light Scattering and Electron Microscopy.** *Int J Mol Sci.* 2021; **22**(23): 12772. [PubMed Abstract](#) | [Publisher Full Text](#) | [Free Full Text](#)
- Meng W, He C, Hao Y, et al.: **Prospects and challenges of extracellular vesicle-based drug delivery system: considering cell source.** *Drug Deliv.* 2020; **27**(1): 585–598. [PubMed Abstract](#) | [Publisher Full Text](#) | [Free Full Text](#)
- Dooley K, McConnell RE, Xu K, et al.: **A versatile platform for generating engineered extracellular vesicles with defined therapeutic properties.** *Mol Ther.* 2021; **29**(5): 1729–1743. [PubMed Abstract](#) | [Publisher Full Text](#) | [Free Full Text](#)
- Dad HA, Gu TW, Zhu AQ, et al.: **Plant Exosome-like Nanovesicles: Emerging Therapeutics and Drug Delivery Nanoplatforms.** *Mol Ther.* 2021; **29**(1): 13–31. [PubMed Abstract](#) | [Publisher Full Text](#) | [Free Full Text](#)
- Garaeva L, Kamyshinsky R, Kil Y, et al.: **Delivery of functional exogenous proteins by plant-derived vesicles to human cells *in vitro*.** *Sci Rep.* 2021; **11**(1): 6489. [PubMed Abstract](#) | [Publisher Full Text](#) | [Free Full Text](#)
- Théry C, Witwer KW, Aikawa E, et al.: **Minimal information for studies of extracellular vesicles 2018 (MISEV2018): a position statement of the International Society for Extracellular Vesicles and update of the MISEV2014 guidelines.** *J Extracell Vesicles.* 2018; **7**(1): 1535750. [PubMed Abstract](#) | [Publisher Full Text](#) | [Free Full Text](#)
- Aaronson S: **The synthesis of extracellular macromolecules and membranes by a population of the phytoflagellate *Ochromonas danica*.** *Limnol Oceanogr.* 1971; **16**(1): 1–9. [Publisher Full Text](#)
- Aaronson S, Behrens U, Orner R, et al.: **Ultrastructure of intracellular and extracellular vesicles, membranes, and myelin figures produced by *Ochromonas danica*.** *J Ultrastruct Res.* 1971; **35**(5–6): 418–430. [PubMed Abstract](#) | [Publisher Full Text](#)
- Billmire EW Jr: **Isolation and Characterization of the Plasma and Extracellular Membranes of *Ochromonas Danica*.** Ph.D. City University of New York; 1974. [Reference Source](#)
- Snell WJ, Clausell A, Moore WS: **Flagellar adhesion in chlamydomonas induces synthesis of two high molecular weight cell surface proteins.** *J Cell Biol.* 1983; **96**(3): 589–597. [PubMed Abstract](#) | [Publisher Full Text](#) | [Free Full Text](#)
- McLean RJ, Laurendi CJ, Brown RM Jr: **The Relationship of Gamone to the Mating Reaction in *Chlamydomonas moewusii*.** *Proc Natl Acad Sci U S A.* 1974; **71**(7): 2610–2613. [PubMed Abstract](#) | [Publisher Full Text](#) | [Free Full Text](#)
- Bergman K, Goodenough UW, Goodenough DA, et al.: **Gametic differentiation in *Chlamydomonas reinhardtii*. II. Flagellar membranes and the agglutination reaction.** *J Cell Biol.* 1975; **67**(3): 606–622. [PubMed Abstract](#) | [Publisher Full Text](#) | [Free Full Text](#)
- Schatz D, Rosenwasser S, Malitsky S, et al.: **Communication via extracellular vesicles enhances viral infection of a cosmopolitan alga.** *Nat Microbiol.* 2017; **2**(11): 1485–1492. [PubMed Abstract](#) | [Publisher Full Text](#)
- Théry C, Amigorena S, Raposo G, et al.: **Isolation and Characterization of Exosomes from Cell Culture Supernatants and Biological Fluids.** *Curr Protoc Cell Biol.* 2006; **30**(1): Chapter 3:Unit 3.22. [PubMed Abstract](#) | [Publisher Full Text](#)
- Guillard RRL: **Culture of Phytoplankton for Feeding Marine Invertebrates.** In: Smith WL, Chanley MH, eds. *Culture of Marine Invertebrate Animals.* Springer US; 1975; 29–60. [Publisher Full Text](#)
- Paterna A, Rao E, Adamo G, et al.: **Isolation of Extracellular Vesicles From Microalgae: A Renewable and Scalable Bioprocess.** *Front Bioeng Biotechnol.* 2022; **10**: 836747. [PubMed Abstract](#) | [Publisher Full Text](#) | [Free Full Text](#)
- Brown W: **Dynamic Light Scattering: The Method and Some Applications.** Clarendon Press; Oxford University Press; 1993. [Reference Source](#)
- Schärtl W: **Light Scattering from Polymer Solutions and Nanoparticle Dispersions.** Springer; 2007. [Publisher Full Text](#)
- Shurer CR, Kuo JCH, Roberts LM, et al.: **Physical Principles of Membrane Shape Regulation by the Glycocalyx.** *Cell.* 2019; **177**(7): 1757–1770.e21. [PubMed Abstract](#) | [Publisher Full Text](#) | [Free Full Text](#)
- Fessler JH, Fessler LI: **Electron microscopic visualization of the polysaccharide hyaluronic acid.** *Proc Natl Acad Sci U S A.* 1966; **56**(1): 141–147. [PubMed Abstract](#) | [Publisher Full Text](#) | [Free Full Text](#)
- Ng L, Grodzinsky AJ, Patwari P, et al.: **Individual cartilage aggrecan macromolecules and their constituent glycosaminoglycans visualized via atomic force microscopy.** *J Struct Biol.* 2003; **143**(3): 242–257. [PubMed Abstract](#) | [Publisher Full Text](#)
- Buckwalter JA, Rosenberg LC: **Electron microscopic studies of cartilage proteoglycans. Direct evidence for the variable length of the chondroitin sulfate-rich region of proteoglycan subunit core protein.** *J Biol Chem.* 1982; **257**(16): 9830–9839. [PubMed Abstract](#)
- Silverman JM, Chan SK, Robinson DP, et al.: **Proteomic analysis of the secretome of *Leishmania donovani*.** *Genome Biol.* 2008; **9**(2): R35. [PubMed Abstract](#) | [Publisher Full Text](#) | [Free Full Text](#)
- Ivošević DeNardis N, Pletikapić G, Frkanec R, et al.: **From algal cells to autofluorescent ghost plasma membrane vesicles.** *Bioelectrochemistry.* 2020; **134**: 107524. [PubMed Abstract](#) | [Publisher Full Text](#)
- Kralj-Iglič V, Pocsfalvi G, Mesarec L, et al.: **Minimizing isotropic and deviatoric membrane energy – An unifying formation mechanism of different cellular membrane nanovesicle types.** *Yi X, ed. PLoS One.* 2020; **15**(12): e0244796. [PubMed Abstract](#) | [Publisher Full Text](#) | [Free Full Text](#)
- György B, Módos K, Pállinger E, et al.: **Detection and isolation of cell-derived microparticles are compromised by protein complexes resulting from shared biophysical parameters.** *Blood.* 2011; **117**(4): e39–e48. [PubMed Abstract](#) | [Publisher Full Text](#)
- Osteikoetxea X, Sódar B, Németh A, et al.: **Differential detergent sensitivity of extracellular vesicle subpopulations.** *Org Biomol Chem.* 2015; **13**(38): 9775–9782. [PubMed Abstract](#) | [Publisher Full Text](#)
- Veronika KI, Zavec Apolonija B, Darja B, et al.: **Scanning electron microscope images of *Dunaliella tertiolecta* and *Phaeodactylum tricorutum* cultures and scanning electron microscope images and cryogenic electron microscope images of isolated small cellular particles from respective conditioned media.** *Zenodo.* 2022. <http://www.doi.org/10.5281/zenodo.6908895>
- Veronika KI, Antonella B, Darja B, et al.: **Raw data on dynamic light scattering assessment of small cellular particles isolated from conditioned culture media of *Dunaliella tertiolecta* and *Phaeodactylum tricorutum*. Effect of Triton X-100 and temperature [Data set].** *Zenodo.* 2022. <http://www.doi.org/10.5281/zenodo.7016692>